CrossMark
← click for updates

Multicomponent sequential polymerizations of alkynes, carbonyl chloride and amino ester salts toward helical and luminescent polymers

Haiqin Deng,[a,b] Engui Zhao,[a,b] Anakin C. S. Leung,[a,b] Rongrong Hu,[c] Yun Zhang,[a,b] Jacky W. Y. Lam*[a,b] and Ben Zhong Tang*[a,b,c]

Multicomponent sequential reactions have recently received much attention owing to their outstanding advantages, such as simple operation, atom economy, and environmental benefit. In this work, we report a new multicomponent sequential reaction and the corresponding multicomponent sequential polymerization approach to construct conjugated structures with advanced functionalities. By employing 1,8-diazabicyclo[5.4.0]undec-7-ene as an additive, alkynes, carbonyl chloride and amino ester salts undergo a one-pot three-component sequential reaction successfully. Similarly, the derived multicomponent sequential polymerizations of diyne, terephthaloyl chloride and amino ester proceed smoothly in a regio- and stereoregular manner and generate conjugated nitrogen-substituted poly(enaminone)s with high molecular weights in satisfactory yields. All the resulting polymers are soluble in common solvents, and possess high thermal stability and good film-forming ability. Interestingly, the incorporation of optically active chiral amino esters as pendants leads to polymeric products with helical rotating backbones, as revealed by their circular dichroism spectra in the solutions and as cast films. With fluorescent tetraphenyl-ethene moieties embedded in the polymer chains, the polymers display a phenomenon of aggregation-enhanced emission. They emit weakly in the solution state, but fluoresce intensely as aggregates. Moreover, the thin films of the polymers exhibit high light refractivity (n = 1.9305–1.5992) in a wide wavelength region (400–1000 nm), which can be readily modulated by UV irradiation. Additionally, the polymeric products with photosensitivity can generate highly resolved two-dimensional luminescent patterns by UV treatment.

Introduction

The development of efficient polymerization methods to access macromolecules with novel structures and unique functionalities has great academic significance and industrial implications. However, most conventional polymerizations employ only one or two monomers, and are not suitable for constructing complicated polymeric structures with multifunctionalities. Multicomponent polymerizations (MCPs), which are derived from the powerful synthetic masterpiece of multicomponent reactions (MCRs),[1] offer new possibilities for the preparation of macromolecules with well-defined structures. Considerable endeavours have been devoted to exploring new MCPs,[2] which leads to increasing reports in the literature.[3] In a typical MCP, several monomers and catalysts are added together and they undergo transformation in one reaction system. Thus, sensible monomer design should be accomplished, in order to avoid interference among the components and diminish side reactions.[4]

To settle the monomer incompatibility issue and expand the general applicability of MCRs as well as MCPs, organic chemists come up with the idea to develop multicomponent sequential reactions,[5] in which the newly formed intermediate without isolation directly undergoes the next reaction *in situ* to afford the desired molecular skeleton. In multicomponent sequential reactions, the reaction components are added in a sequential manner rather than in a one-step fashion. Thus, the potentially interacting components are spatially and temporally separated and side reactions can be diminished, over-

[a]HKUST-Shenzhen Research Institute, No. 9 Yuexing 1st RD, South Area, Hi-tech Park, Nanshan, Shenzhen 518057, China. E-mail: chjacky@ust.hk, tangbenz@ust.hk
[b]Department of Chemistry, Hong Kong Branch of Chinese National Engineering Research Center for Tissue Restoration and Reconstruction, Institute for Advanced Study, Institute of Molecular Functional Materials, Division of Biomedical Engineering, Division of Life Science and State Key Laboratory of Molecular Neuroscience, The Hong Kong University of Science & Technology (HKUST), Clear Water Bay, Kowloon, Hong Kong, China
[c]Guangdong Innovative Research Team, SCUT-HKUST Joint Research Laboratory, State Key Laboratory of Luminescent Materials and Devices, South China University of Technology (SCUT), Guangzhou 510640, China

coming the limitations of common MCRs. This conceptually novel approach stands out with compelling advantages, such as high efficiency, functional group tolerance, atom economy, and diminution of waste production, making it a practically useful organic synthesis method.[6] Accordingly, multicomponent sequential polymerizations are expected to produce a library of complicated macromolecules from simple precursors through simple procedures, which are difficult, if not impossible, to be realized by other synthetic approaches. Up to now, some frontier studies on the development of multicomponent sequential polymerizations have been reported.[7] For example, three-component coupling-hydrothiolation polymerizations of alkynes, aroyl chlorides and thiols were developed to access sulfur-substituted or thiophene-containing conjugated functional polymers.[8]

Recently, Müller *et al.* have reported an efficient one-pot three-component sequential coupling-addition reaction of alkynes, carbonyl chlorides and primary/secondary amines in the presence of $Pd(PPh_3)_2Cl_2/CuI$ to prepare enaminones (Scheme 1).[9] The reaction is stereoselective: secondary amines give *E* isomers as predominant products, whilst primary amines only produce *Z* isomers owing to the formation of intramolecular hydrogen bonds between N–H and C=O groups. Inspired by the high efficiency and stereoselectivity of this reaction, we have successfully developed it into the sequential coupling-hydroamination polymerizations employing common primary/secondary amines.[10] Such sequential polymerization approaches as the coupling-addition polymerizations are excellent synthetic pathways to access functional polymers, *e.g.* optically active polymers, which are gaining increasing attention with potential applications in nonlinear optics, asymmetric electrodes, photonic switching and so forth.[11] Hence, it would be delightful if similar sequential coupling-hydroamination reaction and polymerization pathways with a broad monomer scope, such as optically active amines and their derivatives, can be developed to afford chiral molecular structures.

In this work, we report a three-component sequential reaction, which combines the Sonogashira coupling reaction between alkyne and carbonyl chloride and the hydroamination reaction of optically active amino ester salt to the alkynone intermediate. Making use of commercially available and handy substrates, the corresponding sequential polymerizations of alkynes, carbonyl chloride and amino ester salts proceed smoothly and afford regio- and stereoregular conjugated poly(enaminone)s with high molecular weights in satisfactory yields (Scheme 2). The obtained polymers possess good solubi-
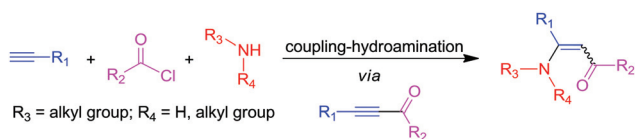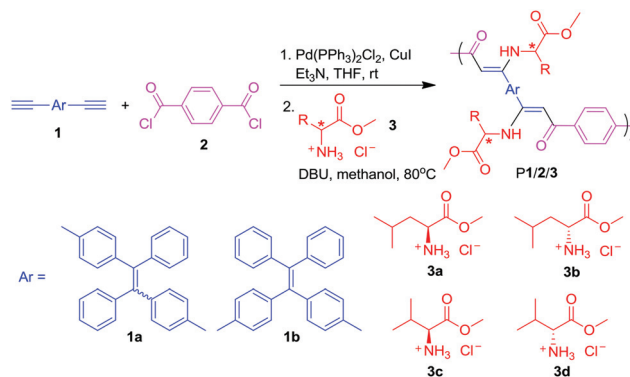
Scheme 2 Synthetic route toward polymers P**1/2/3** by three-component sequential polymerization.

lity and thermal stability, photosensitivity, high and tunable light refractivity, and photopatternability. Interestingly, the polymer backbones are induced to be helically rotated by the chiral amino ester pendants. Moreover, the tetraphenylethene (TPE) moieties embedded in the polymer backbones endow the polymer with a novel aggregation-enhanced emission (AEE) feature.[12] All these attributes enable the polymers to be promising material candidates for high-tech applications.

Results and discussion

Multicomponent sequential reaction

Prior to the exploration of polymerization, we first tested the feasibility of a small-molecule reaction with optically active amino ester salts, following the reported reaction procedures.[9] L-Leucine methyl ester hydrochloride **3a**, TPE-containing monoyne **5** and commercially available benzoyl chloride **6** were employed. First, **5** and **6** were dissolved in tetrahydrofuran (THF) and reacted in the presence of $Pd(PPh_3)_2Cl_2$, CuI and triethylamine (Et_3N) under a nitrogen environment. Afterward, **3a** together with methanol was added into the reaction mixture to undergo the next hydroamination reaction. However, only a trace amount of the desired product was obtained, suggesting that the amino ester salts could not undergo the sequential reaction efficiently under the reported reaction circumstance.[9] Compared with our previous system, the major difference is the replacement of amines with acidic **3a**. Thus, we added excess 1,8-diazabicyclo[5.4.0]undec-7-ene (DBU) along with **3a** into the reaction mixture after completing the coupling reaction between **5** and **6** (Scheme 3). Delight-

Scheme 1 Three-component sequential coupling-hydroamination reaction.

Scheme 3 Synthetic route to model compound **4**.

fully, the hydroamination proceeded smoothly, affording desired product **4** with sole *Z*-conformation, as confirmed by standard spectroscopic techniques, such as ^{1}H NMR, ^{13}C NMR and high resolution mass spectrometry (HRMS).

Multicomponent sequential polymerization

The nice preliminary result of the small-molecule sequential reaction inspired us to develop it into corresponding polymerizations by employing alkynes, carbonyl chloride and amino ester salts as monomers. TPE-containing diynes **1a** and **1b** were prepared by following the procedures reported previously.[13] Terephthaloyl chloride **2** and optically active amino ester salts **3a–d** were commercially available and used as received without further purification. Since the addition of DBU will significantly affect the efficiency of the hydroamination reaction, we systematically investigated its effect on the polymerization. The procedure of typical sequential polymerization of **1a**, **2** and **3a** was similar to our previous report.[10] Catalyzed by Pd(PPh$_3$)$_2$Cl$_2$, CuI and Et$_3$N, **1a** was first reacted with **2** in THF under nitrogen for 15 min at room temperature. Then, **3a** and methanol with/without DBU were added to undergo the hydroamination reaction *in situ* at 80 °C for 24 h (Table 1). Without DBU, the hydroamination is inefficient, yielding poly(alkynone)s as the major product with a trace amount of the desired addition product (Table 1, entry 1). With the increase of the DBU concentration, poly(alkynone)s are transformed into poly(enaminone)s gradually. When the concentrations of DBU and **3a** are equal, only desired poly(enaminone)s with a high molecular weight (M_w = 18 200) (Table 1, entry 5) are obtained in high yield (91%).

To follow the DBU promoted transformation of poly(alkynone)s to poly(enaminone)s, ^{1}H NMR was applied to characterize the polymeric products obtained at different concentrations of DBU (Fig. 1). Without DBU, the polymerization generates products with a predominant alkynone structure (Fig. 1A). The result indicates that the Sonogashira coupling reaction of **1a** and **2** is very efficient to afford the intermediates, but the hydroamination reaction hardly takes place without the addition of DBU (Table 1, entry 1). In the presence of 0.05 M of DBU (Table 1, entry 2), two new reso-
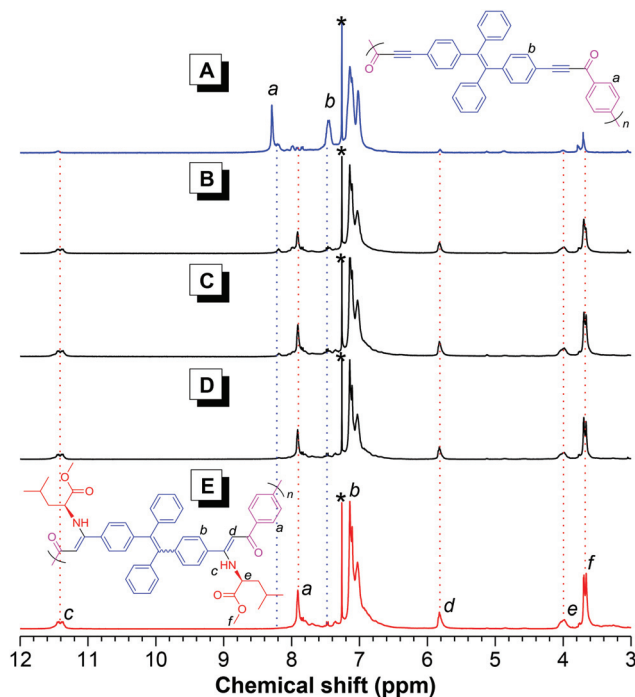

Fig. 1 ^{1}H NMR spectra of the polymeric products obtained from Table 1, (A) entry 1, (B) entry 2, (C) entry 3, (D) entry 4 and (E) entry 5 in chloroform-d, respectively. The solvent peaks are marked with asterisks.

nance peaks associated with the amino proton (c) and vinyl proton (d) of the polymeric product emerge at δ 11.38 and δ 5.83, respectively (Fig. 1B). With the continuous increase of the DBU concentration (Table 1, entries 3 and 4), these two peaks become higher with larger integral areas, whilst the resonance peak associated with aromatic protons (a) is shifted from δ 8.28 to δ 7.91 with gradual decrease of the former peak and increase of the latter one (Fig. 1C and D). When the concentration of DBU is equal to that of **3a** (Table 1, entry 5), the peak associated with a proton located at δ 8.28 is completely disappeared, suggesting the completion of the addition reaction. All the other peaks in Fig. 1E match well with the structure of the desired addition products.

The solvent effect on the polymerization was then investigated and the results are summarized in Table 2. CH$_3$CN and DMF (Table 2, entries 1 and 2) are nonsolvents for the polymerization, producing trace amounts of the desired products. Polymerizations in toluene and 1,4-dioxane (Table 2, entries 3 and 4) afford polymers with high yields (up to 86%), but the weight-average molecular weights (M_w) are only 6700 and 12 300, respectively. Among all the tested solvents, THF is the most appropriate medium for the polymerization, giving a soluble polymeric product with the highest molecular weight (M_w = 18 200) and in the highest yield (91%) (Table 2, entry 5). Thus, THF was chosen as the optimum solvent for further studies.

Afterward, the effect of the monomer concentration was investigated by polymerizing **1a**, **2**, and **3a**, while keeping their ratio constant (Table 3). At relatively high monomer concen-

Table 1 The effect of the additive (DBU) on polymerization[a]

Entry	DBU (M)	Yield (%)	M_w[b]	M_w/M_n[b]
1	0	—		
2	0.05	—		
3	0.10	—		
4	0.15	—		
5	0.20	91	18 200	1.7

[a] [**1a**] = [**2**] = 0.05 M, [**3a**] = 0.20 M, [Pd] = 4 mol%, [Cu] = 8 mol%, [Et$_3$N] = 0.10 M. Monomer **1a** was reacted with **2** for 15 min in THF at room temperature followed by the addition of **3a**, methanol and DBU under N$_2$ in the presence of Pd(PPh$_3$)$_2$Cl$_2$, CuI and Et$_3$N. After the addition of **3a**, the reaction mixture was further reacted at 80 °C for 24 h. [b] Estimated by GPC in THF on the basis of a linear polystyrene calibration.

Table 2 Solvent effect on the polymerization of **1a**, **2** and **3a**[a]

Entry	Solvent	Yield (%)	M_w[b]	M_w/M_n[b]
1	CH$_3$CN	Trace		
2	DMF	Trace		
3	Toluene	86	6700	1.7
4	1,4-Dioxane	85	12 300	1.9
5[c]	THF	91	18 200	1.7

[a] [**1a**] = [**2**] = 0.05 M, [**3a**] = [DBU] = 0.20 M, [Pd] = 4 mol%, [Cu] = 8 mol%, [Et$_3$N] = 0.10 M. Monomer **1a** was reacted with **2** for 15 min in the above solvent at room temperature followed by the addition of **3a**, methanol and DBU under N$_2$ in the presence of Pd(PPh$_3$)$_2$Cl$_2$, CuI and Et$_3$N. After the addition of **3a**, the mixture was further reacted at 80 °C for 24 h. [b] Determined by GPC in THF on the basis of a linear polystyrene calibration. [c] Data taken from Table 1, entry 5.

Table 4 Time course on the polymerization of **1a**, **2** and **3a**[a]

Entry	t (h)	Yield (%)	M_w[b]	M_w/M_n[b]
1	6	82	15 900	1.8
2	12	90	16 500	1.7
3	18	83	17 700	1.8
4[c]	24	91	18 200	1.7
5	30	87	20 800	1.9

[a] [**1a**] = [**2**] = 0.05 M, [**3a**] = [DBU] = 0.20 M, [Pd] = 4 mol%, [Cu] = 8 mol%, [Et$_3$N] = 0.1 M. Monomer **1a** was reacted with **2** for 15 min in THF at room temperature followed by the addition of **3a**, methanol and DBU under N$_2$ in the presence of Pd(PPh$_3$)$_2$Cl$_2$, CuI and Et$_3$N. After the addition of **3a**, the mixture was reacted at 80 °C for the designed period of time. [b] Determined by GPC in THF on the basis of a linear polystyrene calibration. [c] Data taken from Table 1, entry 5.

Table 3 Effect of the monomer concentration on the polymerization of **1a**, **2** and **3a**[a]

Entry	[**1a**] (M)	Yield (%)	M_w[b]	M_w/M_n[b]
1	0.10	Gel		
2	0.08	Gel		
3	0.06	89	19 300	2.0
4[c]	0.05	91	18 200	1.7
5	0.04	87	16 400	1.8

[a] [**2**] = [**1a**], [Et$_3$N] = 2 [**1a**], [**3a**] = [DBU] = 4 [**1a**], [Pd] = 4 mol%, [Cu] = 8 mol%. Monomer **1a** was reacted with **2** for 15 min in THF at room temperature followed by the addition of **3a**, methanol and DBU under N$_2$ in the presence of Pd(PPh$_3$)$_2$Cl$_2$, CuI and Et$_3$N. After the addition of **3a**, the mixture was further reacted at 80 °C for 24 h. [b] Determined by GPC in THF on the basis of a linear polystyrene calibration. [c] Data taken from Table 1, entry 5.

Table 5 Polymerizations employing different monomer combinations[a]

Entry	Monomers	Yield (%)	M_w[b]	M_w/M_n[b]
1[c]	**1a/2/3a**	91	18 200	1.7
2	**1b/2/3a**	91	18 500	1.8
3	**1b/2/3b**	99	22 400	1.8
4	**1b/2/3c**	94	17 100	1.7
5	**1b/2/3d**	91	17 500	1.6

[a] [**1a–b**] = [**2**] = 0.05 M, [**3a–d**] = [DBU] = 0.20 M, [Pd] = 4 mol%, [Cu] = 8 mol%, [Et$_3$N] = 0.1 M. Monomer **1a–b** reacted with **2** for 15 min in THF at room temperature followed by the addition of **3a–d**, methanol and DBU under N$_2$ in the presence of Pd(PPh$_3$)$_2$Cl$_2$, CuI and Et$_3$N. After the addition of **3a**, the mixture was reacted at 80 °C for 24 h. [b] Determined by GPC in THF on the basis of a linear polystyrene calibration. [c] Data taken from Table 1, entry 5.

trations of 0.10 M and 0.08 M, insoluble gels form quantitatively (Table 3, entries 1 and 2). Reducing the monomer concentrations to 0.60 M can slightly suppress the coupling rate, hence giving a soluble polymeric product with a high M_w of 19 300 in 89% yield (Table 3, entry 3). Decreasing the monomer concentration to 0.05 M (Table 3, entry 4) does not affect the reaction very much, affording polymers with M_w of 18 200 in a slightly higher yield of 91%. Further diluting the monomer to 0.04 M still leads to polymeric products with good solubility, albeit in diminished isolation yield (87%) and M_w (16 400).

Furthermore, the effect of the hydroamination reaction time was investigated by using the above optimized conditions (Table 4). At a reaction time of 6 h, the polymerization proceeds efficiently to afford the product with high yield and high M_w (Table 4, entry 1). Raising the reaction time progressively increases the M_w, whereas the M_w/M_n value remains almost the same. After 24 h of polymerization, the reaction yield is highest (91%) (Table 4, entry 4). Further prolonging the reaction time to 30 h does not affect the reaction much. In general, polymerization is very powerful and can furnish polymeric products in a short reaction time with high M_w and small polydispersities in favorable yields.

To test the robustness of this polymerization reaction, different monomer combinations were studied under the optimum conditions (Table 5). Since the properties of **P1a/2/3a** may be influenced by the isomeric TPE moieties in the polymer backbone, monomer **1b** was utilized to polymerize with **2** and **3a**, affording well-defined polymeric product **P1b/2/3a** with a comparable molecular weight (M_w = 18 500) in similar yield. Similarly, polymerizations employing D-leucine methyl ester hydrochloride **3b**, L-valine methyl ester hydrochloride **3c**, or D-valine methyl ester hydrochloride **3d** as the amine source proceeded smoothly, furnishing soluble polymers **P1b/2/3b**, **P1b/2/3c** and **P1b/2/3d** with M_w values of 22 400, 17 100, and 17 500, respectively, and small polydispersities (1.6–1.8) in high yields. We also performed the polymerization under an air atmosphere to confirm whether the polymerization reaction is air sensitive. By employing similar reaction conditions to Table 5 entry 1, the polymerization under air produced a polymeric product with M_w of 9300 and a polydisperisity of 1.5 in 95% yield. It demonstrates the high air tolerance of the sequential coupling-hydroamination polymerization.

Structural characterization

The polymers together with monomers and model compounds were characterized by standard spectroscopic techniques,
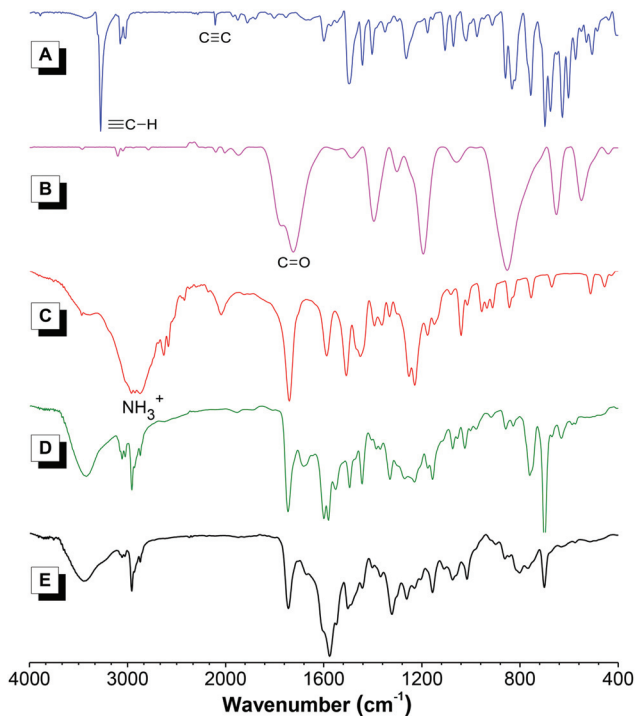
Fig. 2 IR spectra of (A) **1a**, (B) **2**, (C) **3a**, (D) **4** and (E) **P1a/2/3a**.

Fig. 3 ^{1}H NMR spectra of (A) **1a**, (B) **2**, (C) **3a**, (D) **4** and (E) **P1a/2/3a** in CDCl$_3$.

which provided satisfactory analysis data corresponding to the expected molecular structures. The IR and ^{1}H/^{13}C NMR spectra of **1a**, **2**, **3a**, **4** and **P1a/2/3a** are chosen as examples for comparison. In the IR spectrum (Fig. 2) of **1a**, the absorption bands associated with the stretching vibrations of ≡C–H and C≡C are located at 3275 and 2106 cm^{-1}, respectively. Both these absorption bands disappear in the IR spectra of **4** and **P1a/2/3a**, suggesting the complete consumption of the alkyne monomer after the reaction. The result is further verified by the absorption band assignable to the NH^{3+} stretching vibration in **3a** at 2924 cm^{-1}, which also disappears after the addition.

To gain deeper insight into the molecular structures of the polymeric products, their ^{1}H NMR spectra are compared in Fig. 3. The ≡C–H proton (a) of **1a** resonates at δ 3.0, which disappears in the spectra of **P1a/2/3a** and **4**, indicating the occurrence of the sequential reaction. The resonance peak of the aromatic proton (b) of **2** at δ 8.25 is shifted to δ 7.92 in **4** as well as **P1a/2/3a** after the reaction. On the other hand, new peaks at δ 5.83 and δ 11.38 emerge from the spectra of **4** and **P1a/2/3a**, representing the newly formed C=CH group next to the carbonyl group (i proton) and the N–H group (c proton), respectively. The c proton resonance peak is located at a low field, which proves the formation of the intramolecular hydrogen bond between the N–H and C=O groups. Such hydrogen bond can stabilize the Z-vinylene structure and hence avoid the potential enamine/imine tautomerization as well as E/Z isomerization.[14] In addition, **4** and **P1a/2/3a** share similar spectral profiles, but the resonance peaks of the latter are
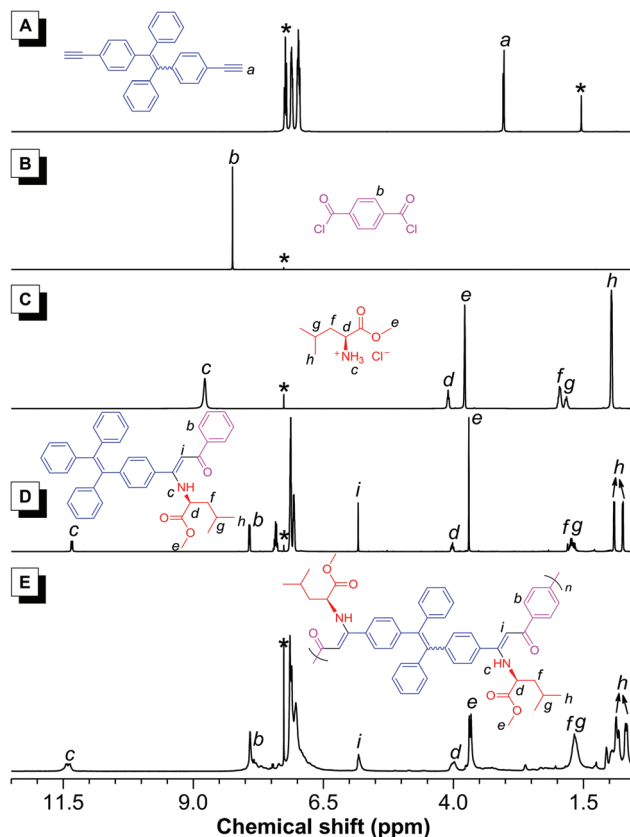
broader than those of the former, owing to its polymeric nature.

Their ^{13}C NMR spectra are shown in Fig. 4. The resonance peak of the triple bond in **1a** at δ 83.9 and δ 77.7 is absent in the spectra of both **4** and **P1a/2/3a**. The carbonyl group resonates at δ 170.8 in **2**, which is shifted to δ 188.1 after the reaction. More convincingly, two new peaks occur at δ 166.1 and δ 93.4 in the spectra of **4** and **P1a/2/3a**, which are associated with the =CAr(N) and =CH(COAr) olefin carbons, respectively. Comparison of the ^{1}H/^{13}C NMR spectra discussed above with our previous work,[10] further discloses an exclusive Z-conformation of the newly formed (N)ArC=CH(COAr) double bond in the skeleton of the resulting polymer, proving its fully regio- and stereospecific structure as shown in Scheme 2.

Solubility and thermal stability

Though the resulting polymers bear conjugated aromatic backbones, they can be well dissolved in THF, DCM, CHCl$_3$ and other common organic solvents, presumably due to the TPE moieties in the polymer backbone. The TPE units with a twisted molecular structure favor a large intermolecular distance and thus create large free volumes to assemble solvent molecules, resulting in the good solubility of the polymers. Thanks to their good solubility, the polymer solutions can be readily fabricated into uniform thin films by a spin-coating
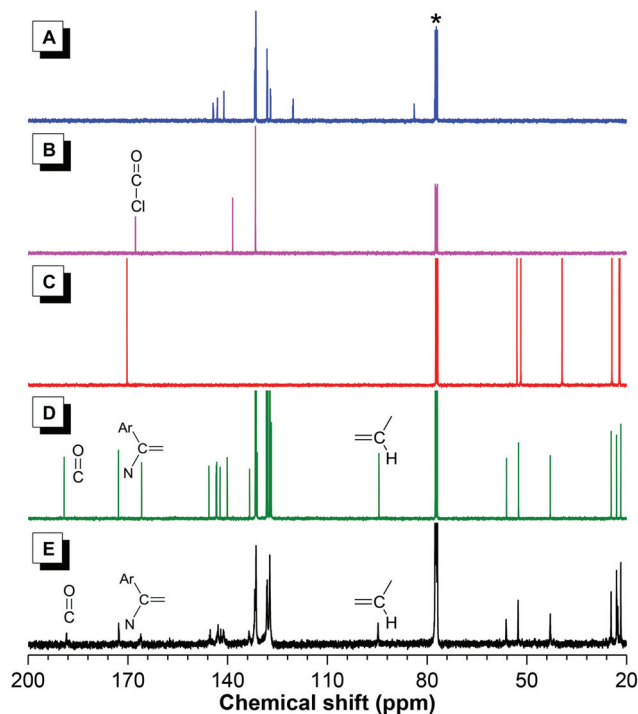
Fig. 4 ^{13}C NMR spectra of (A) **1a**, (B) **2**, (C) **3a**, (D) **4** and (E) P**1a/2/3a** in CDCl$_3$.
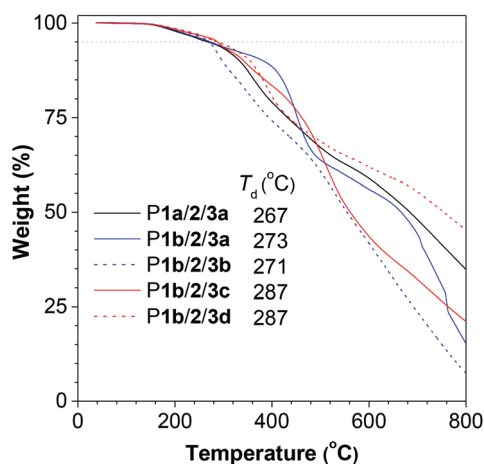

Fig. 5 TGA thermograms of P**1/2/3** recorded under nitrogen at a heating rate of 10 °C min^{-1}.

technique. Their thermal properties were further evaluated by thermogravimetric analysis (TGA) at a temperature range of 50–800 °C. Benefiting from the conjugated skeletons, all the polymeric products possess high thermal stability, with 5% weight loss at temperatures ranging from 267 to 281 °C (Fig. 5).

Light refractivity

Polymers with high refractive indices (*n*) are of great importance in the development of advanced optoelectronic fabrica-
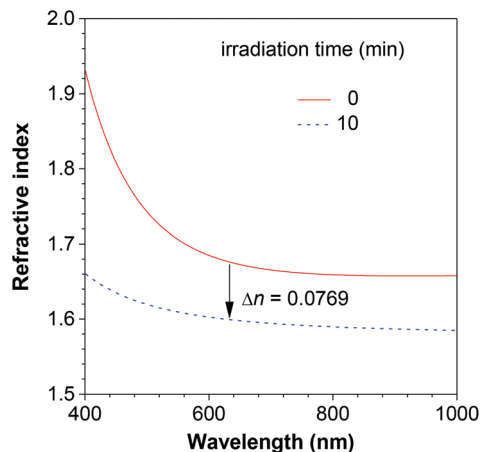

Fig. 6 UV irradiation-induced change of refractivity of the thin film of P**1a/2/3a**.

tions,[15] such as high performance substrates for advanced display devices,[16] antireflective coatings for advanced optical applications,[17] and microlens components for charge-coupled devices.[18] Most conventional organic polymeric materials, including polystyrene, polycarbonate, polyacrylate, poly(methylmethacrylate), *etc.*, demonstrate *n* values within the range of 1.49–1.58,[19] and cannot satisfy the growing demand for materials with high *n* values. Thus, polymer materials with high *n* values are highly desirable. Generally, in the design of materials with high *n* values, two strategies can be considered: one is to incorporate more aromatic rings and heteroatoms and the other is to build a highly polarizable π-conjugation. In this sense, the resulting polymers with plenty of TPE moieties, carbonyl groups, heteroatoms, and a conjugated polymer backbone, are expected to show high *n* values. Thus, P**1a/2/3a** was chosen as an example for refractive index measurement. Thanks to its good film-forming ability, homogeneous thin films on silica wafers can be facilely prepared *via* a spin-coating process. Its film exhibits high *n* values of 1.9305–1.5992 in a wide spectral region of 400–1000 nm (Fig. 6).

Materials with a tunable refractive index are excellent candidates for numerous applications, including optical communication devices and optical data storage.[20] The prepared polymers bear abundant photosensitive groups, and are thus expected to exhibit photo-induced modulation of the refractive index. Taking P**1a/2/3a** as an example, its *n* values drop from 1.9305–1.5992 to 1.6604–1.5849 with a decrease of 0.0769 at 632.8 nm after exposure to UV light for 10 min, demonstrating good refractivity tunability (Fig. 6). This can be ascribed to the UV-assisted photo-oxidative reaction, which changes the chemical structure of the polymer and hence affects the *n* values.

Chiroptical properties

In our previous work, we have demonstrated that incorporating chiral amino acid units or their derivatives into the pendants
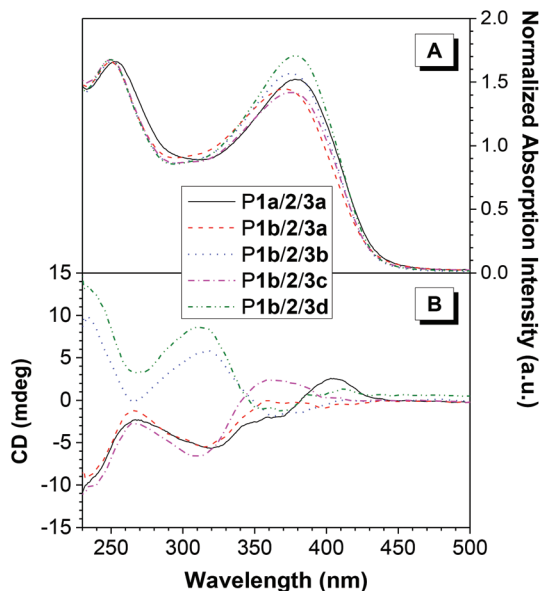
Fig. 7 (A) UV and (B) CD spectra of P1/2/3 in 1,2-dichloroethane solutions; solution concentration: 0.5 mM.

Fig. 8 CD spectra of the cast films prepared by evaporating the 1,2-dichloroethane solution (0.2 mL) of P1b/2/3 at a concentration of 1 mM.

of polyphenylacetylene can induce the polymer to obtain a helical conformation.[21] In this work, the polymers are functionalized with different chiral amino groups and may inherit the chiroptical properties from the amine precursors. Benefiting from the convenience of equipment, UV and circular dichroism (CD) spectra of the polymers were collected together and summarized in Fig. 7 for comparison. All polymers exhibit similar spectral patterns with absorption bands in the range of 230–450 nm and two peaks centered at 250 nm and 380 nm, respectively. The peak at 380 nm is associated with the absorption of the aromatic rings in the polymer backbone (Fig. 7A). In the CD spectra of these polymers (Fig. 7B), absorption bands peaked at ~315 and 365 nm are observed in a similar wavelength range. Since the leucine-/valine-containing units are CD silent with a wavelength longer than 300 nm,[22] such Cotton effect observed at a long wavelength range should stem from the absorption of the polymer backbones. The CD results demonstrate that the chirality of the amino ester pendants is transferred to the main chains and hence the main chains prefer one-handed helical conformation. Particularly, P1a/2/3a with an isomeric structure, which is caused by the TPE core in the backbone, also displays strong CD signals similar to that of P1b/2/3a, suggesting that the polymer obtained from such a sequential polymerization approach can form a helical structure even with intrinsically isomeric conformations.

Afterward, the chiroptical activities of P1b/2/3 in their cast films were examined (Fig. 8). All the polymer films were prepared by natural evaporation of their 1,2-dichloroethane solutions on quartz substrates. P1b/2/3a and P1b/2/3b, which bear L-leucine methyl ester and D-leucine methyl ester, respectively, display almost opposite CD spectral profiles. Similar phenomena are observed in the CD spectra of P1b/2/3c and P1b/2/3d,
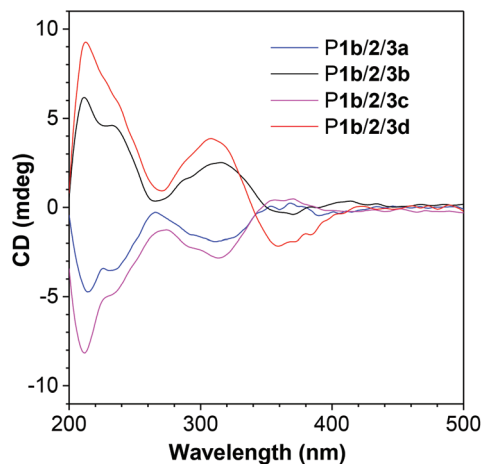
which contain L-valine methyl ester and D-valine methyl ester, respectively. Besides, P1b/2/3a and P1b/2/3c share the same chirality and show similar CD signals. The strong Cotton effect in the range of 260–400 nm, which is associated with the absorption of the polymer backbones, unambiguously confirms the helical conformation of the polymer main chains with a preference for one-handedness.

Light emission

Fluorogens with aggregation-induced emission (AIE) characteristics have recently emerged as a novel class of fluorescent materials with varied applications.[23] The restriction of intramolecular motion was proposed as the main cause for the AIE phenomenon.[24] In this work, we introduce a TPE moiety, a well-known AIE luminogen, into the polymer backbones. The polymers are hence expected to inherit the AIE feature. On the other hand, the embedded TPE moiety is linked to amine moieties by a short spacer, which theoretically represents a typical photo-induced electron transfer (PET) system,[25] as is the case in our previous work.[10b] To verify whether a similar PET effect persists in this system, we systemically studied the emission behaviors of P1a/2/3a in THF/water mixtures with different water fractions (f_w) by means of a spectrofluorometer (Fig. 9). P1a/2/3a can be easily dissolved in THF and is weakly emissive. With the introduction of the poor solvent, water, its emission intensity enhances. Further raising f_w progressively intensifies its light emission. The highest fluorescence intensity is reached at the f_w of 90%, which is 1.91-fold of that in its pure THF solution (Fig. 9B), demonstrating AEE characteristics.

Excited-state intramolecular proton transfer (ESIPT), is a photochemical process, which occurs in the singlet excited state of a molecule with the intramolecular hydrogen bond.[26] Our prepared polymers contain such hydrogen bonds (C=C–N–H⋯O=C) in their conjugation systems. Upon photoexcitation, ESIPT will occur and the molecules are transformed from the keto form to the enol form in the excited state, which
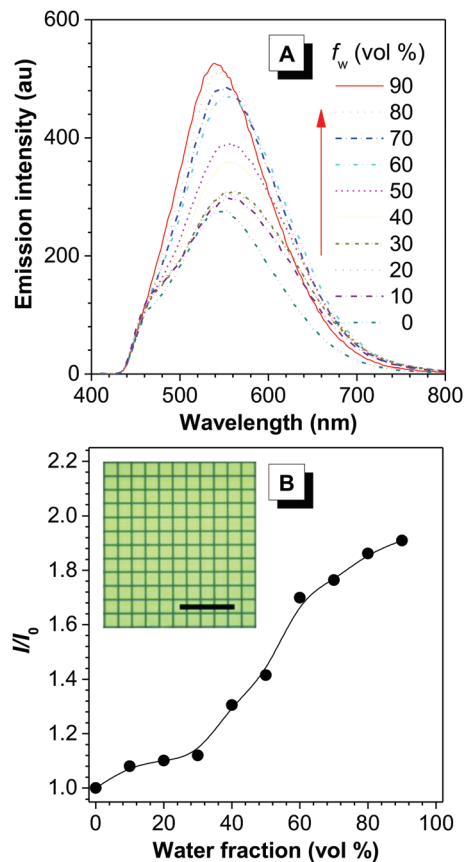
Fig. 9 (A) Emission spectra of P**1a/2/3a** in THF/water mixtures with different f_w (0–90%). Solution concentration: 10 μM; excitation wavelength: 400 nm. (B) Plot of relative emission intensity (I/I_0) *versus* the composition of the aqueous mixture of P**1a/2/3a**. Inset: two-dimensional fluorescent photopattern of P**1a/2/3a**. Excitation wavelength: 330–385 nm; scale bar: 200 μm.

prevents the PET process. Hence, the polymers retain the desired AEE characteristics.

Fluorescent pattern

With photosensitive units embedded in the solid-state emissive polymer skeletons, the polymers are expected to be facilely fabricated into luminescent patterns through a photolithography process. The 1,2-dichloroethane solution of P**1a/2/3a** was first spin-coated on silicon wafers, which was then dried under vacuum at room temperature and irradiated with UV light in an ambient environment for 20 min through a copper photomask. Afterward, the florescent pattern was subjected to observation under a fluorescence microscope. As shown in the inset of Fig. 9B, the discernible luminescent pattern emits green light with regularly arranged grids. The fluorescence of the exposed regions (dark lines) is quenched presumably due to the decomposition of the chromophore caused by the photo-oxidative reaction. The unexposed regions (squares), on the other hand, remain emissive.

Conclusions

In this work, we successfully explored the multicomponent sequential reaction of alkyne, carbonyl chloride and optically active amino ester salt, and developed it into a facile synthetic approach for the construction of functional macromolecules in a sequential manner. Catalyzed by an inexpensive palladium/copper (I) system, the three-component sequential polymerizations proceed efficiently and afford regio- and stereoregular nitrogen-substituted polymeric products with high molecular weights in satisfactory yields. The soluble polymers possess good film-forming ability, satisfactory thermal stability and high refractivity. More importantly, CD signals associated with the Cotton effect are observed in the absorption region of the polymer backbones, demonstrating that the polymer chains are helically rotating in a preferred screw sense owing to the chiral pendants. Moreover, with the TPE units embedded in the polymer backbones, the polymers show AEE behaviors. The thin film of these polymers with strong solid state emission can be fabricated into fluorescent patterns by using photolithographic techniques. Such polymeric materials with CD absorption and strong solid-state emission may demonstrate circularly polarized luminescence properties and are promising candidates for the fabrication of high performance chiroptical devices. Further investigations to explore their chiroptical applications are underway in our lab.

Experimental

Materials

Pd(PPh$_3$)$_2$Cl$_2$ and CuI were purchased from Zhejiang Metallurgical Research Institute Co., Ltd and International Laboratory USA, respectively. Terephthaloyl dichloride, Et$_3$N, methanol, DBU, amino esters and other chemicals and reagents were all purchased from Aldrich, J&K or Merck and used as received. THF was distilled from sodium benzophenone ketyl under nitrogen. Diyne **1a–b** and monoyne **5** were synthesized by following the procedures of the literature.[13]

Instruments

^{1}H/^{13}C NMR spectra were recorded on a Bruker ARX 400 NMR spectrometer using chloroform-d as the solvent and tetramethylsilane (TMS; δ = 0 ppm) as the internal standard. HRMS were performed on a GCT Premier CAB 048 mass spectrometer operated in MALDI-TOF mode. IR spectra were recorded on a PerkinElmer 16 PC FT-IR spectrophotometer. M_w and M_w/M_n of the polymers were estimated by using a Waters Associates gel permeation chromatography (GPC) system equipped with UV detectors. A set of standard polystyrenes covering the M_w range of 10^3–10^7 were utilized for M_w calibration. The polymers were dissolved in THF (~2 mg mL^{-1}), filtered through 0.45 μm PTFE syringe-type filters and then injected into the GPC system by employing THF as the eluent at a flow rate of 1.0 mL min^{-1}.

UV spectra and CD spectra were collected by using a Chira-scan-plus ACD automated circular dichroism spectrometer in a 1 mm quartz cuvette. TGA analysis was performed on a Perkin-Elmer TGA 7 analyzer under a nitrogen atmosphere at a heating rate of 10 °C min⁻¹. PL spectra were recorded on a PerkinElmer LS 55 spectrofluorometer. The polymer films were prepared by spin coating the polymer solutions (~10 mg of polymer in 1 mL of 1,2-dichloroethane) at 800 rpm for 1 min onto silicon wafers, which were then dried in a vacuum oven at room temperature overnight prior to use. For UV induced tuning of the refractivity, the polymer film was irradiated by using a Spectroline ENF-280C/F UV lamp with the incident light intensity of ~18.5 mW cm⁻². The two-dimensional pattern was obtained by UV irradiation of the polymer film through a copper photomask for 20 min and the fluorescence image was collected using a fluorescence microscope (Olympus BX 41) under a UV light source. The n values were collected from a J. A. Woollam M-2000 V multi-wavelength ellipsometer with the range of 400–1000 nm.

Multicomponent sequential reaction

Model compound **4** was prepared from the sequential coupling-hydroamination reaction of TPE-containing monoyne **5**, benzoyl chloride **6** and L-leucine methyl ester hydrochloride **3a** by following a similar procedure to the polymer synthesis. A 10 mL Schlenk tube equipped with a magnetic stirrer was charged with **5** (139 mg, 0.40 mmol), **6** (56 mg, 0.40 mmol), Pd(PPh₃)₂Cl₂ (6 mg, 0.008 mmol), and CuI (3 mg, 0.016 mmol). Afterward, 3.5 mL of THF and 0.06 mL of Et₃N were injected under nitrogen and the mixture was stirred at room temperature for 3 h. **3a** (145.3 mg, 0.80 mmol), DBU (0.12 ml, 0.80 mmol) and 0.5 ml of methanol were added subsequently. The reaction mixture was further stirred for 24 h at 80 °C under nitrogen. Then 20 mL of water was added to quench the reaction and the solution was extracted with 30 mL of DCM for three times. The solvent was evaporated and the crude product was purified by using a silica-gel chromatography column using DCM/hexane (v/v 4/1) as the eluent to give a light yellow solid in 65% yield.

4: IR (KBr), ν (cm⁻¹): 3055, 3024, 2956, 2870, 1745, 1580, 1494, 1330, 1230. ¹H NMR (400 MHz, CDCl₃), δ (TMS, ppm): 11.34 (d, J = 9.7 Hz, 1H), 7.96–7.90 (m, 2H), 7.47–7.38 (m, 3H), 7.19–7.10 (m, 13H), 7.10–7.02 (m, 6H), 5.83 (s, 1H), 4.05–3.99 (m, 1H), 3.70 (s, 3H), 1.83–1.61 (m, 4H), 0.91 (d, J = 6.0 Hz, 3H), 0.74 (d, J = 6.0 Hz, 3H). ¹³C NMR (100 MHz, CDCl₃), δ (TMS, ppm): 189.18, 172.84, 165.86, 145.62, 143.46, 143.40, 143.26, 142.27, 140.12, 140.08, 133.39, 131.71, 131.44, 131.39, 131.10, 128.35, 127.98, 127.95, 127.87, 127.36, 127.22, 126.90, 126.87, 94.48, 56.11, 52.50, 42.95, 24.63, 23.02, 21.73. HRMS (MALDI-TOF): m/z 606.3028 ([M + H]⁺, calcd 606.3003).

Polymer synthesis

Without any special statement, all the polymerizations were carried out under a nitrogen atmosphere by employing standard Schlenk techniques. A typical procedure for the synthesis of **P1a/2/3a** from Table 1, entry 5 is given below as an example.

Into a 10 mL Schlenk tube equipped with a magnetic stirrer were placed TPE-containing diyne **1a** (76 mg, 0.20 mmol), tere-phthaloyl chloride **2** (41 mg, 0.20 mmol), Pd(PPh₃)₂Cl₂ (6 mg, 0.008 mmol), and CuI (3 mg, 0.016 mmol). The Schlenk tube was evacuated under vacuum and flushed with nitrogen for three times. Then 3.5 mL of THF and 0.06 mL of Et₃N were injected into the Schlenk tube. The resulting reaction mixture was stirred for 15 min at room temperature. Afterward, L-leucine methyl ester hydrochloride **3a** (145.3 mg, 0.80 mmol), DBU (0.12 ml, 0.80 mmol) and methanol (0.50 mL, THF/methanol = 7/1) were added into the reaction system. The reaction mixture was further stirred for 24 h at 80 °C under nitrogen and was then added dropwise into 200 mL of methanol *via* a cotton filter to remove the catalyst residue and insoluble substrates formed, if any. The precipitates were collected by filtration and washed with methanol before being dried under vacuum at room temperature to a constant weight.

P1a/2/3a. Yellow powder; 91% (Table 5, entry 1). M_w: 18 200; M_w/M_n: 1.7 (GPC, polystyrene calibration). IR (KBr), ν (cm⁻¹): 3055, 3028, 2957, 2871, 1743, 1575, 1501, 1321, 1261. ¹H NMR (400 MHz, CDCl₃), δ (TMS, ppm): 11.43, 11.39, 7.91, 7.14, 7.11, 7.03, 5.82, 3.69, 3.66, 1.67, 0.87, 0.82, 0.69, 0.67. ¹³C NMR (100 MHz, CDCl₃), δ (TMS, ppm): 188.42, 172.78, 166.12, 145.23, 142.86, 142.07, 141.29, 133.56, 131.83, 131.45, 128.09, 127.33, 94.76, 56.23, 52.63, 42.94, 24.66, 23.03, 22.90, 22.61, 21.73.

P1b/2/3a. Yellow powder; 91% (Table 5, entry 2). M_w: 18 500; M_w/M_n: 1.8 (GPC, polystyrene calibration). IR (KBr), ν (cm⁻¹): 3055, 3028, 2930, 2854, 1743, 1575, 1500, 1323, 1258. ¹H NMR (400 MHz, CDCl₃), δ (TMS, ppm): 11.40, 7.92, 7.12, 7.03, 5.82, 3.99, 3.69, 1.68, 0.86, 0.69. ¹³C NMR (100 MHz, CDCl₃), δ (TMS, ppm): 188.43, 172.78, 143.07, 133.54, 131.83, 131.43, 128.10, 127.38, 94.74, 56.23, 52.65, 42.99, 24.69, 23.06, 22.63, 21.76.

P1b/2/3b. Yellow powder; 99% (Table 5, entry 3). M_w: 22 400; M_w/M_n: 1.8 (GPC, polystyrene calibration). IR (KBr), ν (cm⁻¹): 3055, 3027, 2956, 2871, 1744, 1575, 1502, 1322, 1261. ¹H NMR (400 MHz, CDCl₃), δ (TMS, ppm): 11.38, 7.92, 7.12, 7.03, 5.82, 3.99, 3.70, 1.67, 0.88, 0.69. ¹³C NMR (100 MHz, CDCl₃), δ (TMS, ppm): 188.45, 172.77, 166.08, 145.09, 143.07, 142.07, 133.55, 131.84, 131.42, 128.10, 127.36, 94.73, 56.24, 52.65, 42.96, 24.67, 23.06, 22.63, 21.74.

P1b/2/3c. Yellow powder; 94% (Table 5, entry 4). M_w: 17 100; M_w/M_n: 1.7 (GPC, polystyrene calibration). IR (KBr), ν (cm⁻¹): 3056, 3028, 2964, 2876, 1744, 1576, 1502, 1324, 1266. ¹H NMR (400 MHz, CDCl₃), δ (TMS, ppm): 11.55, 7.93, 7.13, 7.03, 5.85, 3.84, 3.72, 2.17, 0.98, 0.89. ¹³C NMR (100 MHz, CDCl₃), δ (TMS, ppm): 188.43, 171.81, 166.44, 144.87, 143.04, 142.07, 139.21, 133.56, 131.70, 131.42, 128.05, 127.50, 127.33, 94.81, 63.28, 52.33, 32.28, 19.29, 17.86.

P1b/2/3d. Yellow powder; 91% (Table 5, entry 5). M_w: 17 500; M_w/M_n: 1.6 (GPC, polystyrene calibration). IR (KBr), ν (cm⁻¹): 3054, 3027, 2963, 2874, 1743, 1575, 1502, 1323, 1266. ¹H NMR (400 MHz, CDCl₃), δ (TMS, ppm): 11.56, 7.93, 7.13, 7.03, 5.85, 3.84, 3.72, 2.19, 0.98, 0.89. ¹³C NMR (100 MHz, CDCl₃), δ (TMS, ppm): 188.44, 171.83, 166.45, 144.86, 143.06, 142.09,

139.20, 133.56, 131.76, 131.42, 128.01, 127.52, 127.36, 94.85, 63.32, 52.48, 32.30, 19.39, 17.97.

Preparation of nanoaggregates

The stock THF solution of P1a/2/3a with a concentration of 1 mM was first prepared. Then, 0.1 mL of its stock solution was transferred to 10 mL volumetric flasks, followed by the addition of appropriate amounts of THF. Afterward, a poor solvent, water, was added dropwise under vigorous stirring into the THF solution to obtain THF/water mixtures with a concentration of 10 μM and different f_w (0–90 vol%). The emission spectra of the resultant solutions were measured immediately on a spectrofluorometer.

Acknowledgements

Notes and references

1 (a) R. C. Cioc, E. Ruijter and R. V. A. Orru, Green Chem., 2014, 16, 2958–2975; (b) C. de Graaff, E. Ruijter and R. V. A. Orru, Chem. Soc. Rev., 2012, 41, 3969–4009; (c) E. Ruijter, R. Scheffelaar and R. V. A. Orru, Angew Chem., Int. Ed., 2011, 50, 6234–6246; (d) I. Bae, H. Han and S. Chang, J. Am. Chem. Soc., 2005, 127, 2038–2039; (e) S. H. Cho, E. J. Yoo, L. Bae and S. Chang, J. Am. Chem. Soc., 2005, 127, 16046–16047; (f) P. R. Andreana, C. C. Liu and S. L. Schreiber, Org. Lett., 2004, 6, 4231–4233; (g) M. Arend, B. Westermann and N. Risch, Angew Chem., Int. Ed., 1998, 37, 1044–1070; (h) V. A. Peshkov, O. P. Pereshivko and E. V. Van der Eycken, Chem. Soc. Rev., 2012, 41, 3790–3807.

2 (a) Y. Z. Wang, X. X. Deng, L. Li, Z. L. Li, F. S. Du and Z. C. Li, Polym. Chem., 2013, 4, 444–448; (b) O. Kreye, T. Toth and M. A. R. Meier, J. Am. Chem. Soc., 2011, 133, 1790–1792; (c) E. Ihara, Y. Hara, T. Itoh and K. Inoue, Macromolecules, 2011, 44, 5955–5960.

3 (a) I. H. Lee, H. Kim and T. L. Choi, J. Am. Chem. Soc., 2013, 135, 3760–3763; (b) H. Kim and T. L. Choi, ACS Macro Lett., 2014, 3, 791–794; (c) H. Q. Deng, E. G. Zhao, H. K. Li, J. W. Y. Lam and B. Z. Tang, Macromolecules, 2015, 48,

3180–3189; (d) Y. J. Liu, M. Gao, J. W. Y. Lam, R. R. Hu and B. Z. Tang, Macromolecules, 2014, 47, 4908–4919; (e) C. Y. K. Chan, N. W. Tseng, J. W. Y. Lam, J. Z. Liu, R. T. K. Kwok and B. Z. Tang, Macromolecules, 2013, 46, 3246–3256.

4 P. Lundberg, C. J. Hawker, A. Hult and M. Malkoch, Macromol. Rapid Commun., 2008, 29, 998–1015.

5 X. M. Zeng, Chem. Rev., 2013, 113, 6864–6900.

6 J. C. Wasilke, S. J. Obrey, R. T. Baker and G. C. Bazan, Chem. Rev., 2005, 105, 1001–1020.

7 (a) K. Tsuchiya, Y. Shibasaki and M. Ueda, Macromolecules, 2003, 36, 1815–1818; (b) J. W. Chan, C. E. Hoyle and A. B. Lowe, J. Am. Chem. Soc., 2009, 131, 5751–5753; (c) J. P. Zhao, D. Pahovnik, Y. Gnanou and N. Hadjichristidis, Polym. Chem., 2014, 5, 3750–3753.

8 (a) H. Q. Deng, R. R. Hu, E. G. Zhao, C. Y. K. Chan, J. W. Y. Lam and B. Z. Tang, Macromolecules, 2014, 47, 4920–4929; (b) C. Zheng, H. Q. Deng, Z. J. Zhao, A. J. Qin, R. R. Hu and B. Z. Tang, Macromolecules, 2015, 48, 1941–1951.

9 A. S. Karpov and T. J. J. Müller, Synthesis, 2003, 2815–2826.

10 (a) H. Q. Deng, R. R. Hu, A. C. S. Leung, E. G. Zhao, J. W. Y. Lam and B. Z. Tang, Polym. Chem., 2015, 6, 4436–4446; (b) H. Q. Deng, Z. K. He, J. W. Y. Lam and B. Z. Tang, Polym. Chem., 2015, 6, 8297–8305.

11 (a) T. E. Hopkins and K. B. Wagener, Adv. Mater., 2002, 14, 1703–1715; (b) M. M. Green, J. W. Park, T. Sato, A. Teramoto, S. Lifson, R. L. B. Selinger and J. V. Selinger, Angew Chem., Int. Ed., 1999, 38, 3139–3154; (c) J. Z. Liu, J. W. Y. Lam and B. Z. Tang, Chem. Rev., 2009, 109, 5799–5867; (d) C. K. W. Jim, J. W. Y. Lam, C. W. T. Leung, A. J. Qin, F. Mahtab and B. Z. Tang, Macromolecules, 2011, 44, 2427–2437; (e) Y. Okamoto and T. Nakano, Chem. Rev., 1994, 94, 349–372.

12 R. Hu, N. L. C. Leung and B. Z. Tang, Chem. Soc. Rev., 2014, 43, 4494–4562.

13 R. Hu, J. L. Maldonado, M. Rodriguez, C. Deng, C. K. W. Jim, J. W. Y. Lam, M. M. F. Yuen, G. Ramos-Ortiz and B. Z. Tang, J. Mater. Chem., 2012, 22, 232–240.

14 (a) F. Pohlki and S. Doye, Chem. Soc. Rev., 2003, 32, 104–114; (b) T. Muller, K. C. Hultzsch, M. Yus, F. Foubelo and M. Tada, Chem. Rev., 2008, 108, 3795–3892.

15 (a) J.-G. Liu and M. Ueda, J. Mater. Chem., 2009, 19, 8907–8919; (b) E. K. Macdonald and A. P. Shaver, Polym. Int., 2015, 64, 6–14; (c) T. Higashihara and M. Ueda, Macromolecules, 2015, 48, 1915–1929.

16 T. Nakamura, H. Fujii, N. Juni and N. Tsutsumi, Opt. Rev., 2006, 13, 104–110.

17 K. C. Krogman, T. Druffel and M. K. Sunkara, Nanotechnology, 2005, 16, S338–S343.

18 J. L. Regolini, D. Benoit and P. Morin, Microelectron. Reliab., 2007, 47, 739–742.

19 (a) J. Brandrup, E. H. Immergut and E. A. Grulke, Polymer handbook, 4th edn, Wiley, New York, Chichester, 2004; (b) J. E. Mark, Polymer data handbook, Oxford University Press, Oxford, New York, 2009.

20 T. Kopplmayr, M. Cardinale, G. Jakopic, G. Trimmel, W. Kern and T. Griesser, *J. Mater. Chem.*, 2011, **21**, 2965–2973.

21 B. S. Li, K. K. L. Cheuk, F. Salhi, J. W. Y. Lam, J. A. K. Cha, X. D. Xiao, C. L. Bai and B. Z. Tang, *Nano Lett.*, 2001, **1**, 323–328.

22 (*a*) H. Nishino, A. Kosaka, G. A. Hembury, F. Aoki, K. Miyauchi, H. Shitomi, H. Onuki and Y. Inoue, *J. Am. Chem. Soc.*, 2002, **124**, 11618–11627; (*b*) C. Toniolo, *J. Phys. Chem.*, 1970, **74**, 1390–1392; (*c*) H. K. Li, J. Cheng, Y. H. Zhao, J. W. Y. Lam, K. S. Wong, H. K. Wu, B. S. Li and B. Z. Tang, *Mater. Horiz.*, 2014, **1**, 518–521; (*d*) H. K. Li, J. Cheng, H. Q. Deng, E. G. Zhao, B. Shen, J. W. Y. Lam, K. S. Wong, H. K. Wu, B. S. Li and B. Z. Tang, *J. Mater. Chem. C*, 2015, **3**, 2399–2404.

23 Y. N. Hong, J. W. Y. Lam and B. Z. Tang, *Chem. Soc. Rev.*, 2011, **40**, 5361–5388.

24 J. Mei, Y. Hong, J. W. Lam, A. Qin, Y. Tang and B. Z. Tang, *Adv. Mater.*, 2014, **26**, 5429–5479.

25 (*a*) W. Zhang, Z. Ma, L. Du and M. Li, *Analyst*, 2014, **139**, 2641–2649; (*b*) A. P. Silva, T. S. Moody and G. D. Wright, *Analyst*, 2009, **134**, 2385–2393.

26 J. Z. Zhao, S. M. Ji, Y. H. Chen, H. M. Guo and P. Yang, *Phys. Chem. Chem. Phys.*, 2012, **14**, 8803–8817.